JOURNAL OF GUIDANCE, CONTROL, AND DYNAMICS
Vol. 25, No. 5, September–October 2002

Integrated Algorithm for Lunar Transfer Trajectories Using a Pseudostate Technique

R. V. Ramanan*
Vikram Sarabhai Space Center, Thiruvananthapuram 695 022, India

An integrated algorithm to generate the design of one-way transfer trajectories for moon missions is presented. The transfer trajectories are generated by including the gravity fields of the Earth and the moon based on a pseudostate technique. The pseudostate is determined by assuming a rectilinear hyperbola for the arrival phase. The translunar injection state is obtained by an iteration on the argument of latitude of the parking orbit through Lambert problem solutions. Certain advantages of this algorithm are discussed. The Lambert solution is obtained by using Battin's universal algorithm. The numerical results obtained using this algorithm are analyzed and a comparison with the Lambert conic solutions is made. The error in achieving the target with the Lambert conic solution is quantified. The role of the pseudostate solution in reducing the error is discussed. The reduction in the error in achieving the target position is found to be more than 95%.

Nomenclature

a_p, a_t	=	semimajor axis of the parking orbit, transfer orbit, respectively, km
d_1	=	date of departure
e_p, e_t	=	eccentricity of the parking orbit, transfer orbit
F	=	hyperbolic eccentric anomaly
i_p, i_t	=	inclination of the parking orbit, transfer orbit, deg
$\overline{\boldsymbol{R}_M}$	=	position vector of the moon, km
$\overline{\boldsymbol{R}'_M}$	=	pseudostate vector of the moon, km
$\overline{\boldsymbol{R}_p}$	=	position vector of translunar injection (TLI) on the parking orbit, km
r_h	=	radial distance of the space vehicle from moon's center at $d_1 + (t - \Delta t)$, km
t	=	flight duration, days
u_p	=	argument of latitude of the TLI on the parking orbit $(\omega_p + v_p)$, deg
$\overline{V_t}$	=	velocity after TLI, km/s
$\overline{\boldsymbol{V}_A}$	=	arrival velocity vector of the space vehicle at $d_1 + t$, km/s
$\overline{\boldsymbol{V}_M}$	=	orbital velocity vector of the moon, km/s
$\overline{\boldsymbol{V}_\infty}$	=	hyperbolic excess velocity vector, km/s
v_h	=	velocity of the space vehicle at $d_1 + (t - \Delta t)$, km/s
v_p, v_t	=	true anomaly on the parking orbit, transfer orbit corresponding to the TLI, deg
$\boldsymbol{\alpha}_M$	=	right ascension of the moon measured from the first point of Aries counterclockwise to the projection of the position vector of the moon onto the Earth's equator, deg
$\boldsymbol{\alpha}_\infty$	=	right ascension of the hyperbolic excess velocity vector in lunar equator and equinox of date coordinate frame, deg
Δt	=	duration over which the lunar gravity field is active on the space vehicle, days
ΔV	=	impulse required for TLI, km/s
$\boldsymbol{\delta}_M$	=	declination of the moon measured along the perpendicular from the position to the Earth's equator, deg
$\boldsymbol{\delta}_\infty$	=	declination of the hyperbolic excess velocity vector in lunar equator and equinox of date coordinate frame, deg
θ_∞	=	asymptotic angle between the departure radius vector and $\overline{\boldsymbol{V}_\infty}$, deg
μ_M	=	gravitational constant of the moon, km^3/s^2
Ω_p, Ω_t	=	right ascension of ascending node of the parking orbit, transfer orbit, deg
ω_p, ω_t	=	argument of perigee of the parking orbit, transfer orbit, deg

Received 9 July 2001; revision received 21 February 2002; accepted for publication 4 March 2002.

*Scientist, Applied Mathematics Division.

I. Introduction

In the planning of lunar/interplanetary missions, establishing the transfer trajectory design is the first and foremost requirement. The space vehicle, in such missions, passes through multiple gravity fields, which makes the trajectory design more complex. In general, the trajectory design involves three major phases: departure hyperbolic trajectory phase relative to the departure planet, interplanetary transfer trajectory phase relative to the central body, and approach trajectory phase relative to the target planet. These three phases must be synchronized to realize a mission. First, the interplanetary phase is obtained by treating the target planets as point masses, and then, the determined conditions are transformed into asymptotic conditions relative to the departure planet. The departure phase is designed to achieve these asymptotic conditions. Departure escape trajectories are achieved by proper choice of the parking orbit characteristics. The approach trajectories are obtained by selecting an appropriate aim point satisfying the arrival constraints. Typically a large number of iterations must be carried out on these three phases to synchronize them. For lunar missions, because the moon's sphere of influence (with respect to the Earth) lies within the Earth's sphere of influence (with respect to the sun), only two phases are required for the trajectory design. The departure phase and the cruise phase are combined into a single phase, and the parking orbit characteristics are determined to achieve this combined phase trajectory. In the literature, although many algorithms are presented for interplanetary transfer trajectories, an algorithm to design lunar transfer trajectories is not readily available. In this paper, an integrated algorithm based on pseudostate theory to design the combined lunar transfer trajectories is presented. A new approach that determines the parking orbit characteristics, such as the parking orbit orientation and the location on the parking orbit where translunar injection is initiated by imparting the required impulse, and that is also uniformly valid for all types of parking orbits, for example, circular or elliptical, is followed in the algorithm. The imparting of an impulse is assumed to be instantaneous. The necessity for such an algorithm is discussed with an overview of the pseudostate theory development and its application in the context of interplanetary missions discussed in the literature. A comparison with Lambert's conic method (point conic method) is also made to establish the accuracy levels obtained with this algorithm.

II. Pseudostate Theory and Its Evolution

Several methods exist to design the transfer trajectories, and they can be grouped into three main categories: 1) patched conic methods, 2) pseudostate-theory-based methods, and 3) search by numerical integration. The only accurate method to design such transfer trajectories under multiple gravity fields is a numerical one because there is no known closed-form solution to the n-body equations of motion. This method is expensive and computationally intensive because it involves an exorbitant number of simulations. Also, the convergence depends on the initial guess of the initial state. Other methods such as point conic and patched conic techniques ignore the presence of multiple gravity fields or consider them one at a time to design the transfer trajectory through the sphere of influence concepts. In the patched conic method, the relative velocity vectors are matched at the patch points on the sphere of influence by iteration. The initial state obtained through these methods, when propagated under realistic force models, deviates from the actual transfer trajectory and fails to meet the required mission objectives. The pseudostate theory solves the problem by correcting the major portion of the error occurring due to patched/point conic approaches without actually employing a search by numerical integration.

The evolution of the pseudostate theory started with Wilson's paper[1] in 1970. As described in his paper, the pseudostate theory to study the motion of a space vehicle under the gravitational influences of two bodies (termed as primary body and secondary body) is outlined as follows:

1) Given an initial state, propagate the trajectory to the desired time (at which the state of a space vehicle is to be found under the influence of two bodies) as a conic relative to the primary body only.

2) Transform the primary-centered state to a state with respect to the secondary body.

3) Propagate back along a straight line with the velocity vector with respect to the secondary body to the initial time to find the secondary-centered position of the space vehicle that would have been in the absence of the primary-body gravity field.

4) Propagate forward to the desired time as a conic relative to the secondary body.

The new state thus obtained is equivalent to the state that would have been obtained by simulating the trajectory numerically from the initial state under the influence of the gravity fields of both the bodies. Byrnes and Hooper[2] developed the multiconic method, a rapid propagation method, based on the pseudostate theory as a substitute for the numerical integration retaining nearly the same level of accuracies. When the step sizes for the desired time are small, these methods equal the numerical integration method for the three-body equations of motion.

Designing the trajectory in the presence of the multiple gravity fields of the two target planets can be considered as a three-body Lambert problem. The preceding multistep propagation technique was modified into a one-step method to solve this three-body Lambert problem by Byrnes.[3] In this technique the three-body Lambert problem is converted into a two-body Lambert problem of connecting two states, namely, the departure state and a pseudostate (corresponding to a target aim point) in a fixed time. Unlike in the multiconic method, the backup propagation time is not the same as the forward propagation time, but a fixed time is chosen during which the secondary-body gravity field is assumed to be active in addition to the central force field. Also the approach trajectory characteristics to the target aim point, generally a hyperbola, are obtained through iteration together with an iteration for the transfer trajectory. This technique, as presented, is more suitable to handle gravity-assist trajectories around the secondary body, and it has to be modified to just flyby the secondary body, that is, one-way transfer meeting some target constraints.

The target constraints create the additional complexity of fixing an aim point and the characteristics of an approach trajectory for the solution process. To avoid this complication, Sergeyevskey et al.[4] introduced a simplification on the approach trajectory characteristics by assuming that it is a rectilinear hyperbola. Because the periapsis of a rectilinear hyperbola is the center of the secondary body and the eccentricity is one, the target aim point gets fixed. This partial knowledge about the approach trajectory avoids the iteration required to obtain the hyperbolic characteristics. Sergeyevskey et al. have presented an algorithm that generates transfer trajectories for interplanetary missions. This method, in addition to its simplicity due to the assumption on the approach trajectory, improves the initial conditions and, hence, the transfer trajectory by correcting the major portion of errors of the point conic method and offers better initial guesses for a precision trajectory-generation process, which reduces the number of iterations required to achieve convergence. Because the algorithm is presented as applicable to interplanetary transfer trajectories, the requirements of the parking orbit conditions such as the ascending node of the injection plane and the location of transplanetary injection to attain the transfer trajectory design are not discussed.[4] In general, this problem is tackled separately in interplanetary missions because it offers such flexibility.

III. Lunar Transfer Trajectory Design

In the design of lunar transfer trajectories such flexibility is not available because the moon (secondary body) lies within the sphere of influence of the Earth (primary body) itself. In the case of interplanetary missions, the orbit transfer is carried out between the orbits of the planets, and hence, the initial position of the space vehicle is the same as the position of the Earth, which can be obtained from ephemeris data for the selected departure time, and the parking orbit requirements are computed based on the departure asymptotic conditions. Battin, in Ref. 5, Sec. 11.5, presents a mathematical formulation to obtain circular parking orbit characteristics achieving the departure asymptotic conditions (the right ascension and declination of the $\overline{V}_\infty$). The information about the turn angle θ_∞ is used to locate the transplanetary injection point. A strategy used in the Mars Observer Mission, as discussed by Bell et al.[6] consists of finding the transplanetary injection point from an elliptic parking orbit. The strategy searches along the parking orbit for a location, minimizing the incremental velocity required to achieve the asymptotic conditions.

For a lunar mission, the transfer is carried out between the parking orbit and the orbit of the moon. The initial state on the parking orbit is unknown, and it is to be found along with the transfer trajectory design by iteration. The absence of the departure asymptotic conditions for a lunar mission necessitates a different treatment for translunar injection to meet the requirement that the parking orbit plane should contain the target point (the state of the moon) at the time of injection. Although the search technique along the parking orbit could be followed to find the translunar injection (TLI) location, this involves the solution of a Lambert problem for each point on the parking orbit, which results in a large computational time. Battin (Ref. 5, Sec. 9.3) presented an algorithm to arrive at parking orbit requirements for circumlunar trajectories based on the patched conic techniques that could possibly be modified for one-way transfer trajectories. The algorithm does not allow the flight time to exceed the flight time needed for a parabolic conic connecting the positions and, hence, puts a restriction on the type of conic (only elliptic orbits). Newton iteration is used to arrive at the transfer angle and, hence, the location for TLI. With the exception of this work, the literature is scanty on this topic.

In this paper, an integrated approach to obtain parking orbit conditions for TLI and the transfer trajectory design is presented together with elaborate algorithmic details. The algorithm presents a unified approach in finding the location of TLI for both circular and elliptical parking orbits. The solution of the three-body Lambert problem is obtained by finding a pseudostate with respect to the moon and by solving the two-body Lambert problem involving the departure state and the pseudostate. The algorithm uses the universal algorithm by Battin[5] to solve the two-body Lambert problem, an unified approach uniformly valid for all types of orbits. When the rectilinear pseudostate technique[4] is combined with the universal algorithm,[5] this algorithm derives advantages from both. The universal algorithm usage for the Lambert problem solution allows us to design any type of transfer trajectories, namely, circular, elliptical, parabolic, and hyperbolic. Two iterations are involved on two states: one on the departure state and another one on the pseudostate corresponding to the aim point. Also the information that the injection for the lunar journey takes place at the perigee of the transfer trajectory is

derived. Although it is redundant for tangential, horizontal injection where the parking orbit and transfer trajectory lie in the same plane and the injection takes place in the horizon plane, it might be useful for conducting nontangential, nonhorizontal injection studies that require out-of-plane as well as in-plane maneuvers before injection.

IV. Integrated Algorithm

The steps of the integrated algorithm are as follows:

1) Fix the following inputs: date of departure d_1, flight duration t, a duration during which the moon's gravity field also acts on the space vehicle, for example, Δt, semimajor axis, eccentricity, and inclination of the parking orbit.

2) Find the geocentric position of the moon with respect to the Earth's equator on arrival $(d_1 + t)$ using lunar ephemeris data, and set the pseudostate vector $\overline{\boldsymbol{R}'_M} = \overline{\boldsymbol{R}_M}$.

3) Compute the right ascension and declination of $\overline{\boldsymbol{R}'_M}$ with respect to the Earth's equator.

4) Compute the right ascension of the ascending node of the parking orbit using the equations given in Appendix A.

The procedure to find the location on the parking orbit by iteration to initiate TLI starts here. That, for a tangential injection, the argument of perigee of the transfer orbit has to be equal to the argument of latitude of the parking orbit at TLI is utilized in step 8. The iteration on this parameter through repeated Lambert problem solutions makes it possible for the algorithm to find the location of TLI on both types of parking orbits, namely, circular and elliptical.

5) Assume a value for true anomaly, guess a value for the argument of perigee of the parking orbit, and set $u_p = \omega_p + v_p$.

6) Find the position, $\overline{\boldsymbol{R}_p}$, corresponding to the assumed parking orbit location described by $(a_p, e_p, i_p, \Omega_p, u_p)$.

7) Solve the Lambert problem connecting two positions $\overline{\boldsymbol{R}_p}$ and $\overline{\boldsymbol{R}'_M}$ for flight duration t and obtain the transfer orbit characteristics $(a_t, e_t, i_t, \Omega_t, \omega_t, v_t)$. (Evidently $\Omega_p = \Omega_t$, $i_p = i_t$, and $v_t = 0$. Although this information is known before the start of the iteration, these are again determined by solution of the Lambert problem, thus becoming a verification for the Lambert problem solution procedure.)

8) Replace $\omega_p + v_p$ of the parking orbit by ω_t with the other parking orbit characteristics remaining the same.

9) Find the new position $\overline{\boldsymbol{R}_p}$ corresponding to the updated characteristics on the parking orbit.

10) Repeat steps 7–9 until the two successive values of ω_t differ only by a very small tolerance.

11) Find the arrival velocity $\overline{\boldsymbol{V}_A}$ of the space vehicle on the transfer trajectory.

12) Find the hyperbolic excess velocity $\overline{\boldsymbol{V}_\infty}$ as $\overline{\boldsymbol{V}_A} - \overline{\boldsymbol{V}_M}$ and $\boldsymbol{\alpha}_\infty$ and $\boldsymbol{\delta}_\infty$.

The internal iteration to obtain the parking orbit characteristics ends here. The method consisting of the preceding steps is often referred to as the point conic method or Lambert conic method in the literature. If the lunar gravity field is ignored, the solution is arrived at the end of step 12. The pseudostate technique that corrects the trajectory by including the lunar gravity field is presented in the following steps and the iteration to find out the pseudostate starts.

13) Find the radial distance r_h and velocity v_h along the rectilinear hyperbola at $(t - \Delta t)$ with V_∞, Δt, and μ_M as inputs using the procedure described in Appendix B. Set an indication that the pass is the first one.

14) Because, for a rectilinear hyperbola, radial and velocity directions are parallel, find $\overline{r_h}$ and $\overline{v_h}$ as $\overline{r_h} = r_h(\overline{V_\infty}/V_\infty)$ and $\overline{v_h} = v_h(\overline{V_\infty}/V_\infty)$.

15) Sweep back from $(\overline{r_h}, \overline{v_h})$ in a straight line with constant velocity v_h for a duration of Δt and compute the new pseudostate as $\overline{r'_M} = \overline{r_h} - \overline{v_h}\Delta t$ in the selenocentric frame and as $\overline{\boldsymbol{R}'_M} = \overline{\boldsymbol{R}_M} + \overline{r'_M}$ in the geocentric frame.

16) If the pass is not the first one for the current iteration, then proceed to step 3 with the new $\overline{\boldsymbol{R}'_M}$. Otherwise compute the time of travel $\Delta t'$ from $\overline{r_h}$ to the periapsis of the rectilinear hyperbola with the velocity as $\overline{\boldsymbol{V}_\infty}$. (Use the equations given in Appendix C.)

17) Find the time difference $\epsilon_t = |\Delta t - \Delta t'|$. If ϵ_t is less than a prefixed tolerance, the solution is reached. Otherwise proceed to step 18.

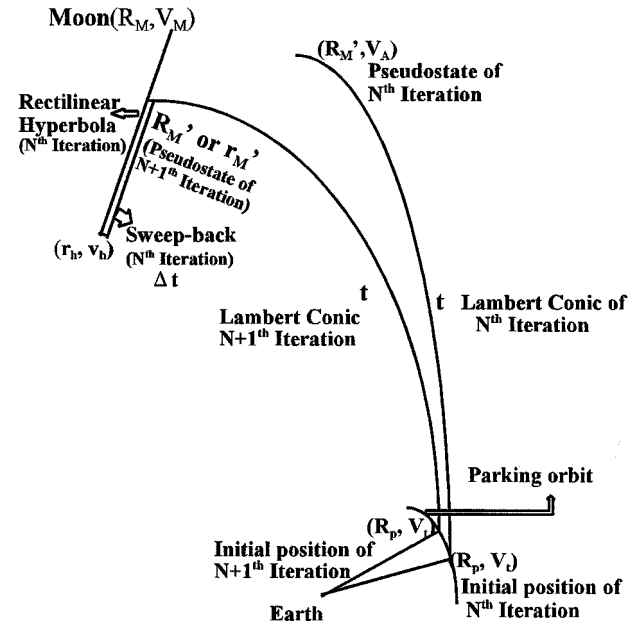

Fig. 1 Geometry of pseudostate lunar transfer trajectory.

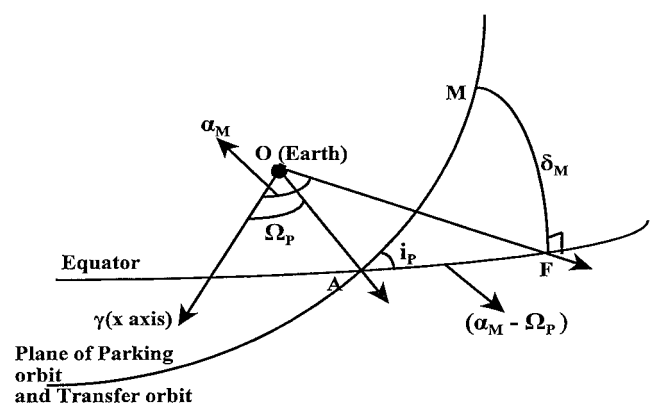

Fig. 2 Geometry of parking and transfer orbit orientation.

18) Find the correction to the pseudostate; let $\partial r_h/\partial t = v_h$ if this is the first iteration. Otherwise compute

$$\frac{\partial r_h}{\partial t} = \frac{r_h - r_{h\,\text{old}}}{\epsilon_t - \epsilon_{t\,\text{old}}}$$

19) Correct the asymptotic distance (r_h) by $r_h = r_h + (\partial r_h/\partial t)\epsilon_t$ and reset the old values to the current values with an indication that the pass is not the first one for the current iteration.

20) Repeat steps 14 onward until ϵ_t is less than a prefixed tolerance.

In a typical external iteration, steps 13–20 are executed, and then again 14–16 are executed. With the transfer of the internal iteration to step 3, this typical external iteration ends. Figure 1 shows the geometry of the pseudostate algorithm. The two iterations in this procedure, the first one (internal iteration) to obtain the location of TLI on the parking orbit and the second one (external iteration) to obtain the pseudostate, are repeated until the convergence criteria on ϵ_t is satisfied. The process of convergence typically requires about four to five iterations on both internal and external iterations. The geometry of the parking and transfer orbit orientation is shown in Fig. 2.

V. Illustration and Analysis

The outlined algorithm has been implemented, and illustrative results with the analysis are presented in this section. The size of the parking orbit is selected as 300 km circular, and the inclination is fixed at 45 deg. A flight duration of 5 days is assumed for the mission, and the period for departure is chosen as January–February 2007, covering about two orbital periods of the moon. The departure

is characterized by incremental velocity, right ascension of ascending node of the parking orbit, and an argument of latitude on the parking orbit for TLI. The arrival is characterized by the hyperbolic excess velocity and the right ascension and declination of the excess velocity vector with respect to the lunar equator.

Generally, as also in this algorithm, in the pseudostate technique, the accuracy of the solution is linked to the parameter sweepback duration. The accuracy levels can be improved by handling this parameter judiciously. The importance of this parameter is discussed by Sweetser.[7] He derived empirical formulas to compute the optimal sweepback duration for interplanetary missions. However, with the flight duration for a lunar mission only 4–5 days, the optimal sweepback duration can be found by varying the sweepback durations from 0 to 5 days in small steps. Obviously, the zero sweepback duration corresponds to the solution by the point conic method. The solutions obtained by the pseudostate technique with different sweepback durations are propagated numerically under a force field consisting of both the Earth and the moon, and the errors in the end constraint, namely reaching the target aim point in a prescribed flight duration, are assessed. The variations in the solutions with respect to sweepback duration are shown in Figs. 3 and 4, and its impact on the end constraints, obtained by numerically integrating the solutions under a force model including the Earth and the moon, is shown in Figs. 5 and 6. Figures 3–6 correspond to a departure date of 17 January 2007, which requires minimum energy for TLI in the selected lunar cycle. A comparison of Figs. 3–6 shows that even the small differences (less than 2 deg) in the TLI angles, such as longitude of ascending node and argument of perigee, results in huge errors in the end constraints. The error due to the point conic solution, which ignores lunar gravity field, is about 5.5 h in flight duration when the target is reached or 25,000 km in the target distance after the specified flight duration. The inclusion of the lunar gravity field in the trajectory design process improves the solution in satisfying the end constraints. Even an assumption of a nominal presence of the moon (for about only 0.5 day) reduces the errors in achieving the target drastically (about 50%). Both the TLI angles increase almost linearly after an initial rapid increase. The errors keep reducing until an optimal sweepback duration is reached, and beyond this value, the errors tend to increase again. For these departure conditions, the value is about 75% of the total flight duration, namely, 3.75 days. A further analysis for other departure dates with different relative geometry scenario and for other flight durations has also shown the optimal sweepback duration to be around this percentage value. It

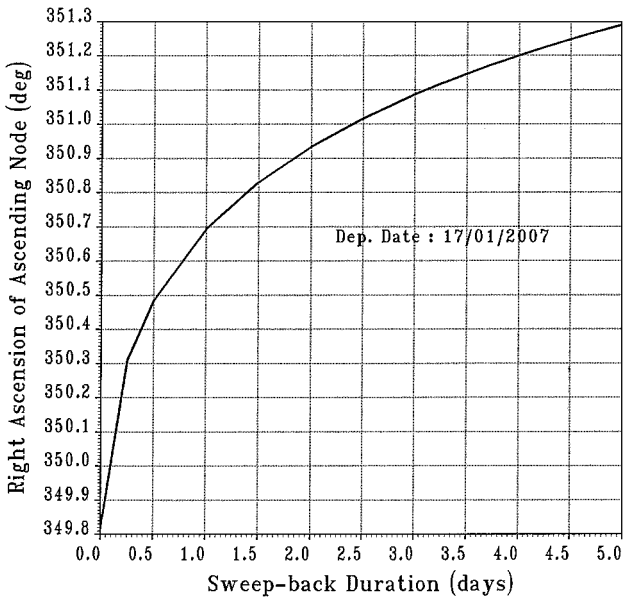

Fig. 3 Parking orbit orientation variation with respect to the sweepback duration.

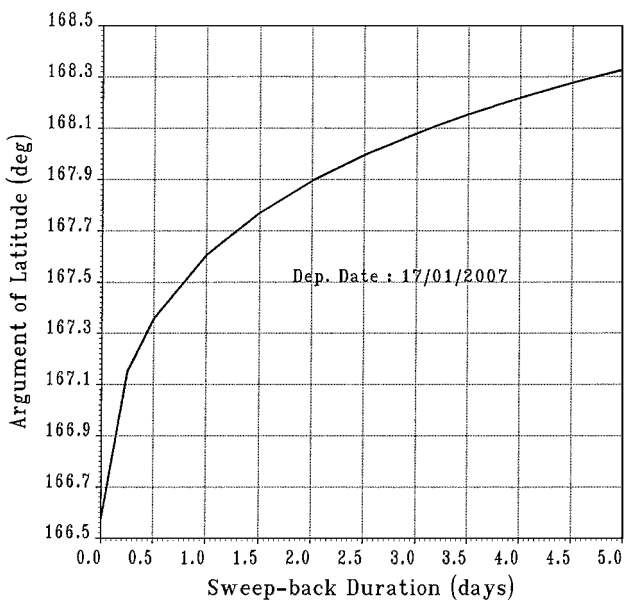

Fig. 4 TLI location variation with respect to the sweepback duration.

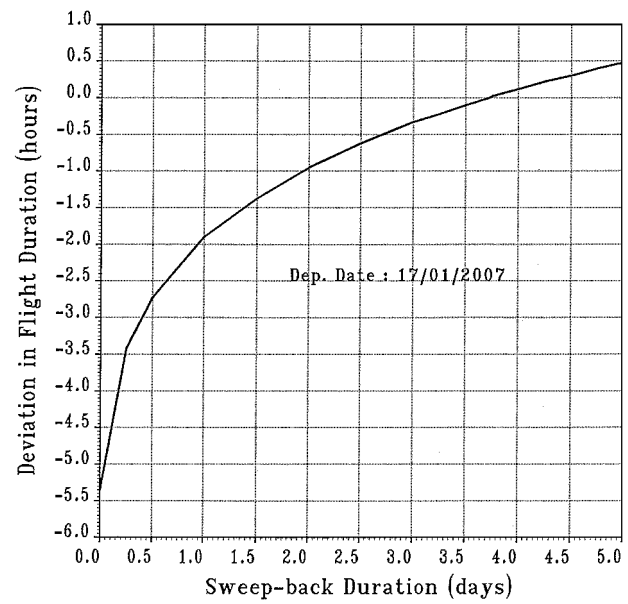

Fig. 5 Deviation in flight duration on reaching the target distance.

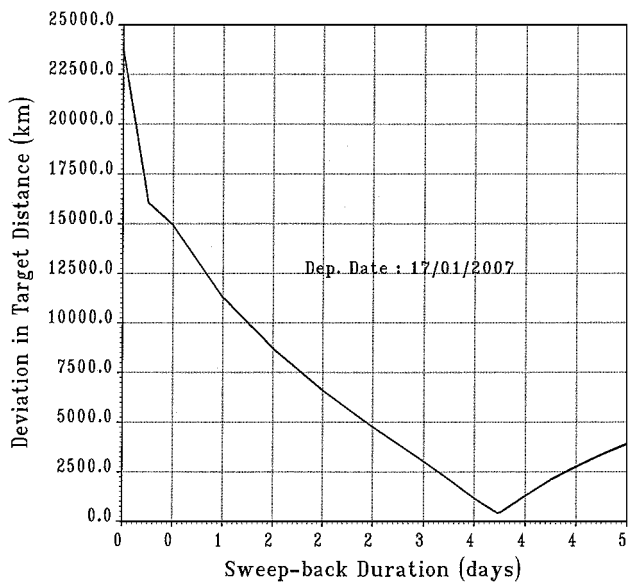

Fig. 6 Deviation from target distance at the specified flight duration.

can safely be concluded that a solution by the pseudostate technique assuming the moon's presence for about 75% of the total duration yields a better solution and meets the end constraints of the transfer trajectory.

Typical lunar mission characteristics obtained using this algorithm are given in Table 1 and comparison is made with the Lambert conic results. The initial state by the pseudostate technique when propagated numerically under the gravity fields of the Earth and the moon for the full flight duration reaches a minimum distance of 423 km from the target aim point in the specified arrival time. Although the algorithm generates impact trajectories, the target aim point can be shifted appropriately to achieve the other nonimpact mission objectives. The incremental velocity requirement does not vary between the techniques, but the angles vary by about 2 deg. As already pointed out, the point conic initial state, when propagated numerically, results in an error of nearly 5.5 h in arrival time, and the space vehicle is at a very large distance from the target aim point at the prescribed time.

The variations of departure characteristics over two lunar orbital periods are shown in Figs. 7–9. The near exact repetition of the characteristics in subsequent lunar cycles is due to the recurrence of the relative geometry. The incremental velocity varies over one lunar orbital period by only about 10 m/s, with minimum and maximum impulse requirements corresponding to the moon's position near perigee and apogee, respectively, at the time of arrival. The right ascension of ascending node varies between 0 and 360 deg, and the argument of latitude varies in the range 180 ± 42 deg in this period.

Table 1 Typical lunar transfer trajectory characteristics and comparison[a]

Parameter	Pseudostate	Lambert conic
V_t, km/s	10.8285	10.8281
ΔV, km/s	3.10278	3.10236
$\Omega_p = \Omega_t$, deg	351.172	349.817
$u_p = \omega_t$, deg	168.184	166.576
a_t, km	188,242.060	187,437.809
e_t	0.96452	0.96437
V_∞, km	0.89250	0.88830
α_∞, deg	−102.526	−102.524
δ_∞, deg	−1.331	−1.269
Closest approach time, day, hr	22 Jan. 2007, 00:00	21 Jan. 2007, 18:39
Closest approach distance, km	−1,315.08	−1,482.328
Distance (km) on 22 Jan. 2007, 00:00 hr	−1,315.08	23,691.32

[a]Departure date on 17 Jan. 2007, 0 h, 0 min, 0 s; flight duration 5 days.

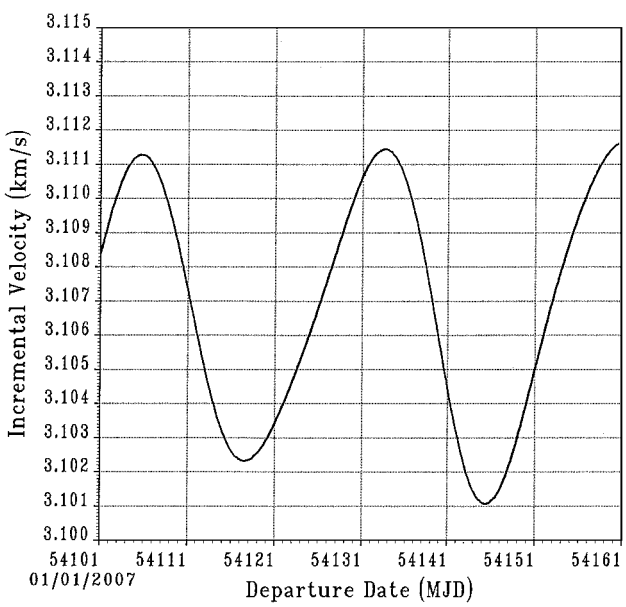

Fig. 7 Profile of the incremental velocity at departure.

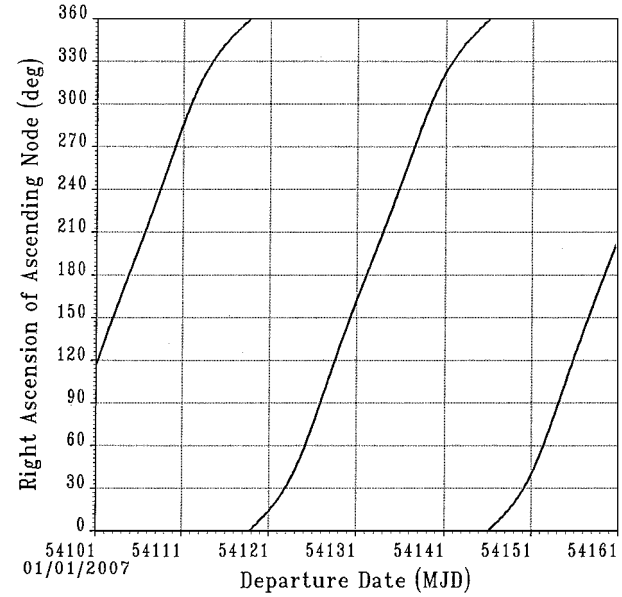

Fig. 8 Profile of right ascension of ascending node of the parking orbit during TLI.

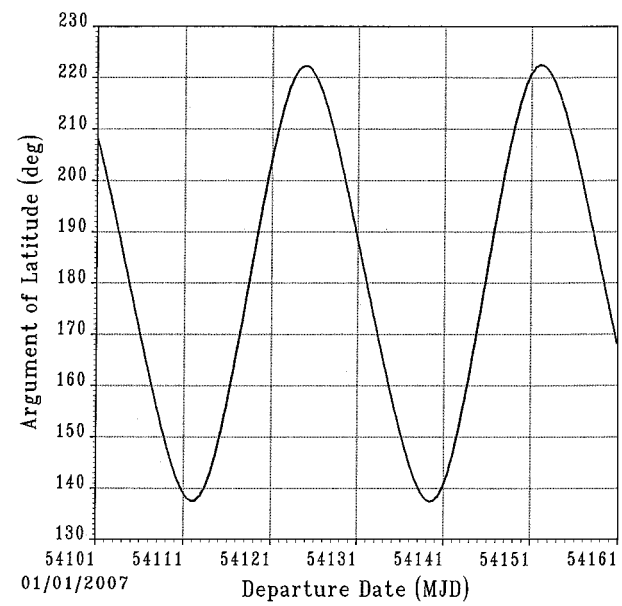

Fig. 9 Profile of argument of latitude of the TLI location.

This amplitude varies drastically with a change in inclination of the parking orbit. For example, for an inclination of 30 deg, this amplitude is about 75 deg. Only one of the two solutions is plotted. The second solution also exhibits similar trends in the variations. The arrival characteristics are plotted in Figs. 10–12. The differences between the solutions of pseudostate and point conic techniques are plotted in Figs. 13 and 14 for departure and arrival characteristics, respectively. The error with respect to the incremental velocity at departure is negligible. The errors in the argument of latitude of TLI fluctuate between −2.0 and +1.5 deg. The right ascension of ascending node deviates in the range 1.3–4.0 deg, indicating that the pseudostate always moves away from the moon's orbit as seen from the x axis. The deviation is maximum when the moon is near its apogee and minimum when the moon is near perigee on arrival. It is also observed that the absolute deviation in u is maximum when the moon is near the Earth's equator, and the deviation is near zero when the moon is near its maximum absolute declination. The impact of the lunar gravity field on the arrival excess velocity is about 8 m/s, and the variation in the angles that fixes the direction of arrival excess velocity is only marginal.

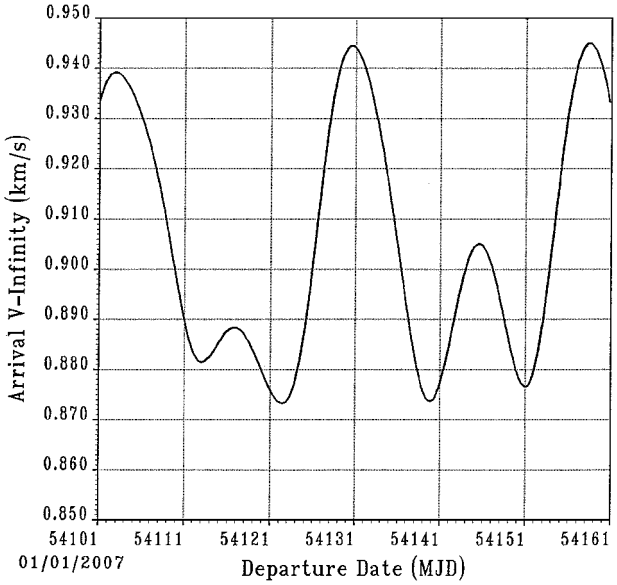

Fig. 10 Variation of hyperbolic excess velocity on arrival.

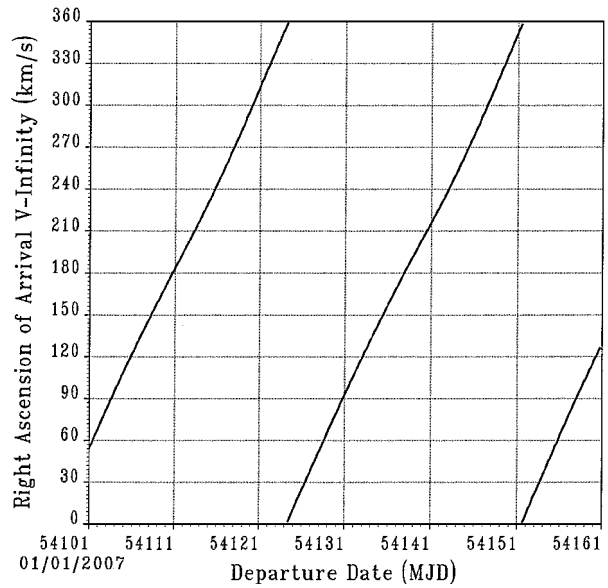

Fig. 11 Variation of right ascension of excess velocity vector.

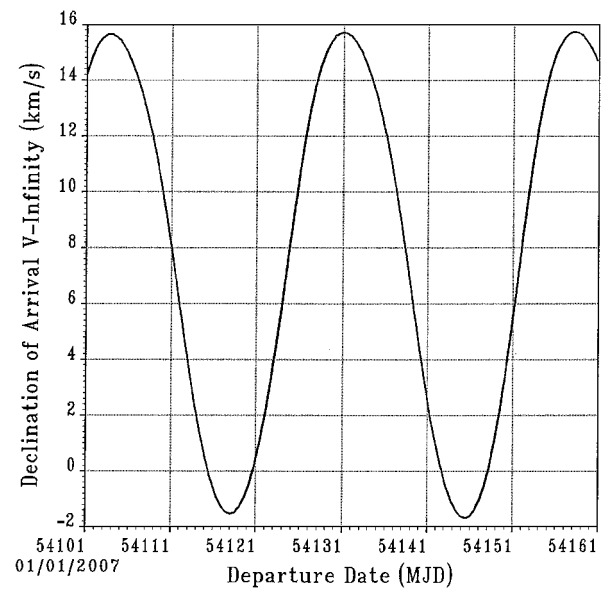

Fig. 12 Variation of declination of excess velocity vector.

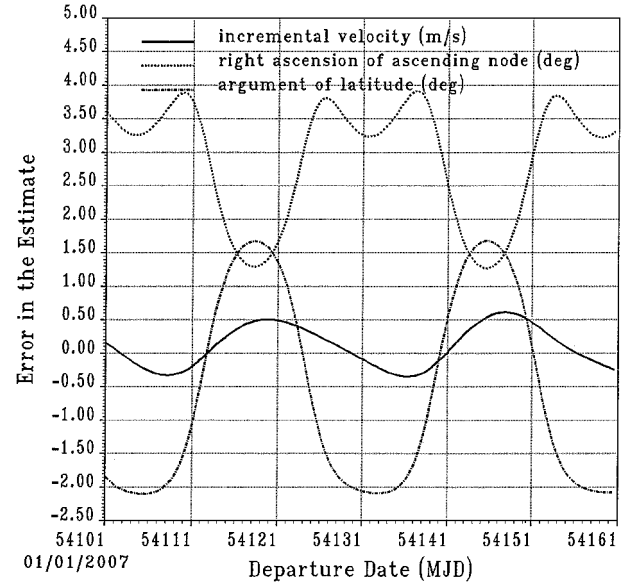

Fig. 13 Differences (pseudo-Lambert) in the departure characteristics.

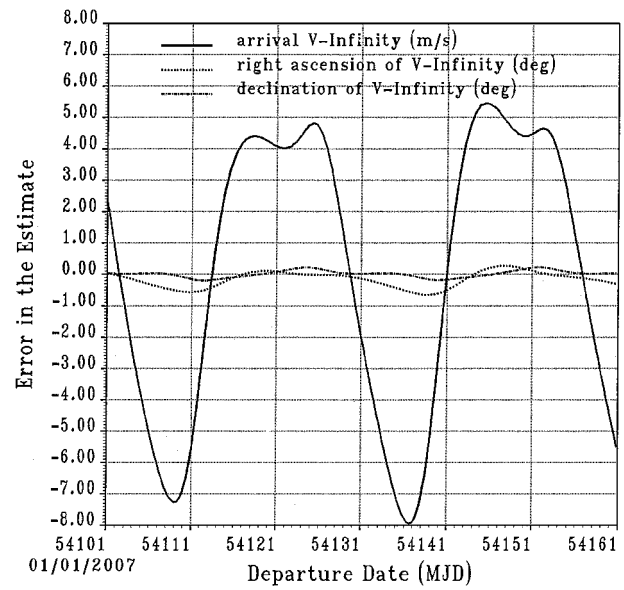

Fig. 14 Differences (pseudo-Lambert) in the arrival characteristics.

VI. Conclusion

An integrated algorithm to obtain the transfer trajectory design together with the required parking orbit characteristics for an impact one-way lunar mission is presented. This algorithm is uniformly valid for circular as well as for elliptical parking orbits and generates any type of lunar transfer trajectories, such as elliptic, hyperbolic, etc. This algorithm provides better data compared to point conic methods, forming a good basis for preliminary lunar mission design analysis with minimum computational effort. The illustrative results are presented and analyzed. The accuracy levels of the algorithm is demonstrated. The importance of the sweepback duration in the context of the present algorithm is highlighted.

Appendix A: Ascending Node of Parking Orbit (Compare Figure 2)

The plane of parking orbit/transfer orbit is chosen such that the initial departure state and the position or pseudoposition of the moon at the time of arrival lies in this plane. Two such planes can be chosen when $|\delta_M| < i_p$, one containing the moon in the ascending phase and the other in the descending phase.

Use of Napier's formula in the spherical triangle AMF of Fig. 2 results in

$$\sin(\alpha_M - \Omega_p) = \tan\delta_M / \tan i_p$$

The second plane is given by

$$\sin[180 - (\alpha_M - \Omega_p)] = \tan \delta_M / \tan i_p$$

Appendix B: Asymptotic Parameters of a Hyperbola

Given V_∞ and Δt, the mean motion is found from

$$n_h = V_\infty^3 / \mu_M$$

The mean anomaly is given by

$$M_h = -n_h \Delta t$$

The eccentric anomaly F is obtained by solving the hyperbolic form of Kepler's equation:

$$M_h = \sinh(F) - F$$

The asymptotic radial distance and velocity are given by

$$r_h = \left(\mu_M / V_\infty^2\right)[\cosh(F) - 1], \qquad v_h = -(\mu_M / r_h v_\infty) \sinh(F)$$

Appendix C: Duration of Travel on a Hyperbola

Given V_∞, r_h and μ_M, the semimajor axis is given by

$$1/a_h = \left| V_\infty^2 / \mu_M - 2/r_h \right|$$

and the eccentric anomaly is obtained from

$$\sinh(F) = \left(r_h v_h / \sqrt{\mu_M}\right)\sqrt{1/a_h}, \qquad F = \log(\sinh F + \cosh F)$$

$$n_h = \sqrt{-\mu / a_h^3}, \qquad M_h = \sinh F - F, \qquad \Delta t = M_h / n_h$$

Acknowledgments

The author acknowledges the encouragement given by V. Adimurthy, P. V. Subba Rao, and S. R. Tandon of Vikram Sarabhai Space Center. He expresses his sincere thanks to the reviewers for the comments and observations.

References

[1] Wilson, S. W., Jr., "A Pseudostate Theory for the Approximation of Three-Body Trajectories," AIAA Paper 70-1061, Aug. 1970.

[2] Byrnes, D. V., and Hooper, H. L., "Multiconic: A Fast and Accurate Method of Computing Space Flight Trajectories," AIAA Paper 70-1062, Aug. 1970.

[3] Byrnes, D. V., "Application of Pseudostate Theory to the Three-Body Lambert Problem," *Journal of the Astronautical Sciences*, Vol. 37, No. 3, 1989, pp. 221–232.

[4] Sergeyevsky, A. B., Byrnes, D. V., and D'Amario, L. A., "Application of the Rectilinear Impact Pseudostate Method to Modeling of Third-Body Effects on Interplanetary Trajectories," AIAA Paper 83-0015, Jan. 1983.

[5] Battin, R. H., *Introduction to the Mathematics and Methods of Astrodynamics*, AIAA Education Series, AIAA, New York, 1987, Secs. 9.3, 11.5.

[6] Bell, S. C., Ginsburg, M. A., and Rao, P. P., "Monte Carlo Analysis of the Titan III/Transfer Orbit Stage Guidance System for the Mars Observer Mission," AIAA Paper 93-3889, 1993.

[7] Sweetser, T. H., "Some Notes on Applying the One-Step Multiconic Method of Trajectory Propagation," *Journal of the Astronautical Sciences*, Vol. 37, No. 3, 1989, pp. 233–250.